Simulation of ^{27}Al MQMAS NMR Spectra of Mordenites Using Point Charge Model with First Layer Only and Multiple Layers of Atoms†

Seen Ae Chae, Oc Hee Han,* and Sang Yeon Lee‡

*Analysis Research Division, Daegu Center, Korea Basic Science Institute, Daegu 702-701, Korea. *E-mail: ohhan@kbsi.re.kr*
‡Department of Applied Chemistry, Kyungpook National University, Daegu 702-701, Korea
Received June 27, 2007

The ^{27}Al multiple quantum magic angle spinning (MQMAS) nuclear magnetic resonance (NMR) spectra of mordenite zeolites were simulated using the point charge model (PCM). The spectra simulated by the PCM considering nearest neighbor atoms only (PCM-n) or including atoms up to the 3rd layer (PCM-m) were not different from those generated by the Hartree-Fock (HF) molecular orbital calculation method. In contrast to the HF and density functional theory methods, the PCM method is simple and convenient to use and does not require sophisticated and expensive computer programs along with specialists to run them. Thus, our results indicate that the spectral simulation of the ^{27}Al MQMAS NMR spectra obtained with the PCM-n is useful, despite its simplicity, especially for porous samples like zeolites with large unit cells and a high volume density of pores. However, it should be pointed out that this conclusion might apply only for the atomic sites with small quadrupole coupling constants.

Key Words : ^{27}Al MQMAS, Solid-state NMR, Mordenite, Point charge model, Si/Al ratio

Introduction

The location of the catalytically active sites in a given zeolite can differ according to the spatial distribution of the Al atoms over the available tetrahedral sites (T sites) in the given lattice, since the Al atoms at the T sites are known to behave as Brönsted acid sites.[1,2] ^{27}Al magic angle spinning (MAS) nuclear magnetic resonance (NMR) has been one of the main techniques used to probe the local structures of the Al sites in zeolites, which are known to be closely correlated with the physical and chemical properties.[2-5] Recently, the multiple quantum MAS (MQMAS) NMR spectra with higher resolution than simple MAS NMR spectra have been employed to resolve the ^{27}Al peaks resulting from the different sites[6-11] by removing the 2nd order quadrupole line broadening.[12,13]

The peak assignment of ^{27}Al MAS or MQMAS NMR spectra is typically carried out by spectral simulation or comparison with the spectra of model compounds. ^{27}Al is a quadrupole nucleus with a spin number of 5/2 and, hence, ^{27}Al NMR spectra are mainly governed by quadrupole interactions with quadrupole parameters such as the quadrupole coupling constant (C_Q) and asymmetry parameter (η). As a result, ^{27}Al NMR spectra can be simulated at a given magnetic field, provided that both the isotropic chemical shifts (δ_i) and the quadrupole parameter values are known, as was recently done for the ^{27}Al MQMAS NMR spectra of ZSM-5 zeolites.[11]

The quadrupole parameters can be derived from the structural parameters by calculation methods such as the ab initio Hartree-Fock (HF) molecular orbital calculation,[14] the density functional theory (DFT),[14-17] or the point charge model (PCM).[11,18] The HF and DFT calculations require sophisticated software programs and experts to run them, whereas the PCM does not. If the quadrupolar parameter values derived from the PCM are similar to those given by the HF or the DFT, then the PCM provides a much more efficient and convenient method of attaining the same goal. Even with the PCM, however, it is preferable to consider as small a number of point charges as possible.

In this work, the quadrupole parameters of Al at 4 different T sites in mordenite zeolite (MOR) with various Si/Al ratios were calculated by the PCM with the 4 nearest neighbor oxygen atoms only (PCM with the first layer only: PCM-n) or with the 20 atoms up to the 3rd layers (PCM with multiple layers: PCM-m) being taken into consideration. The results were compared with those obtained by the HF method as well as with the experimental data. The pros and cons of these two PCM methods were discussed. MORs were selected for the study since they have only 4 crystallographically different T sites (T1, T2, T3, and T4),[19] thereby simplifying the calculation and ^{27}Al NMR spectra. However, the generally low crystallinities of MORs might deteriorate the spectral resolution. MORs have been extensively used as catalysts in petroleum processes.[1]

Experimental

The single crystal XRD data of MOR-4.7 from reference 19 and the neutron powder diffraction data of MOR-5.6 and MOR-10 from reference 20 were used for the calculation of the quadrupole parameters, where the number (*i.e.* x in MOR-x) refers to the Si/Al ratio in the MOR. The coordinates of the atoms surrounding each T site were taken from the unit cell obtained with the Ortep-3 program and the

†This paper is dedicated to Professor Sang Chul Shim on the occasion of his honorable retirement.

observed Al was assumed to sit at the origin (0, 0, 0). For the PCM-n calculation, only the nearest 4 oxygen atoms were considered, while for the PCM-m, the nearest 4 oxygen atoms, 4 silicon atoms connected to the 4 oxygen atoms, and 12 additional oxygen atoms bonded to the silicon atoms were included. The point charge at each atomic site was varied in steps of 0.5 from −0.5 to −2 for oxygen and from 0.5 to 4 for silicon relative to the unit charge for a positron of 1.60×10^{-19} coulombs. The quadrupole parameters, C_Q and η, obtained by the PCM methods and the δ_i values calculated from the mean T-O-T angle (θ) using the equation, δ_i (in ppm) = $-0.50\theta + 132$,[21] were taken to simulate the ^{27}Al MQMAS NMR spectra.[11]

For the HF method, cluster models were built for the different T sites, since the unit cell of MOR was too big to calculate. The cluster models were assumed to have the same structure as that obtained from the XRD data and were not allowed to relax. The cluster models included the atoms up to the 3rd layer. The oxygen in the 3rd layer was assumed to have a chemical bond to a hydrogen atom with a bond length of 0.9575 Å, which is equal to the equivalent distance in a water molecule. The 6-31G* basis set was used. The gauge including atomic orbitals (GIAO), electric field gradients, and natural population analysis options were used for the calculations of the chemical shifts, the nuclear quadrupolar coupling constants, and the atomic charges, respectively. To compare the calculated chemical shifts directly with the experimental data, the calculated chemical shift for each T site in MOR was calibrated using the difference between the calculated and the experimental chemical shifts for Al in the AlH_4^{-1} anion.[15] The HF calculations were carried out using the Gaussian 98 program.[22]

MOR-6.5 (CBV10A in their catalog) was purchased from the Zeolyst International (USA) and used as-received to obtain the ^{27}Al MQMAS NMR spectra on an INOVA 600 MHz system (Varian Inc., U.S.A) with a 14.1 Tesla wide-bore magnet and a CP-MAS probe equipped with 4mm zirconia rotors. Samples were spun at 12.5 kHz with a spin rate fluctuation less than ± 4 Hz and a pulse repetition delay of 2 s. The spectral widths for the F2 and F1 dimension were 200 and 50 kHz, respectively. Among the possible multiple quantum transitions, triple quantum transitions were detected. The first and second hard pulses were 4 and 1.4 μs, respectively, while the third soft pulse length for zero quantum transition filtering was 17 μs. t1 was incremented in steps of 20 μs up to 1262 μs starting from an initial value of 2 μs. For the individual t1 data, 96 transients were accumulated. In addition to the ordinary double Fourier transformation for the 2D data, shearing was applied. This shearing amount for triple quantum transitions is 19:12 = F2:F1 for ^{27}Al nuclei of I = 5/2.[23] The chemical shifts were referenced to those of an external 1 M $AlCl_3$ aqueous solution.

Results and Discussion

The mean T-O-T angles for the individual T sites in MOR-4.7, 5.6, and 10 and the δ_i values derived from them[21] are summarized in Table 1. The upper part of Table 2 shows the quadrupole parameters (C_Q and η) obtained by the PCM-n and PCM-m calculations and the rest of the table presents the δ_{CG1} and δ_{CG2} values calculated from C_Q, η, and δ_i. δ_{CG1} and δ_{CG2} are the shifts of the center of gravity on the F1 and F2 axes, respectively, and are defined as below[23] where ω_o is the carrier frequency of the observed nuclei, and ω^{2Q} is the 2nd order quadrupole shift of the center of gravity of the central (−1/2 ↔ 1/2) transition line:[23]

$$\delta_{CG1} = k_{1k}\delta_i + k_{2k}(\omega^{2Q}/\omega_o),$$

where $k_{1k} = -17/31$ and $k_{2k} = 10/31$ for the triple quantum transition of nuclei with I = 5/2,

$$\delta_{CG2} = \delta_i + (\omega^{2Q}/\omega_o).$$

Point charges of −1 and +2 for oxygen and silicon, respectively, were used for the calculation on the presumption of covalent bonding.

Although the C_Q values, estimated by the PCM-n and PCM-m methods, in Table 2 are not the same, the ^{27}Al MQMAS NMR spectra shown in Figure 1 are practically indistinguishable. The spectra were simulated with the δ_i values in Table 1 and the δ_{CG1} and δ_{CG2} values in Table 2. Our results indicate that the PCM-n method is good enough to simulate the ^{27}Al MQMAS NMR spectra. Indeed, the simulated ^{27}Al MQMAS NMR spectrum for MOR-4.7 could be reasonably aligned with the experimental spectrum of MOR-6.5, as shown in Figure 2. However, this good agreement of the experimental and the simulated spectra might be simply fortuitous. All of the Al sites happen to have a relatively small C_Q value, which results in the ^{27}Al MQMAS NMR spectra being mainly determined by δ_i and

Table 1. Mean T-O-T angles and ^{27}Al isotropic chemical shifts for different T sites in MOR-4.7, MOR-5.6, and MOR-10

	MOR-4.7		MOR-5.6		MOR-10	
Possible Al site	mean T-O-T Angle[a] (°)	δ_i[b] (ppm)	mean T-O-T Angle[c] (°)	δ_i[b] (ppm)	Mean T-O-T Angle[c] (°)	δ_i[b] (ppm)
T1	150.4	56.8	149.0	57.5	149.3	57.4
T2	158.1	53.0	152.8	55.6	153.0	55.5
T3	153.9	55.1	154.8	54.6	155.0	54.5
T4	152.3	55.9	154.0	55.0	153.0	55.5

[a]The T-O-T angles from reference 19 were used for the calculation; [b]^{27}Al isotropic chemical shifts, δ_i, were calculated from the mean T-O-T angles (θ) using the equation, δ_i (in ppm) = $-0.50\theta + 132$ in reference 21; [c]The T-O-T angles from reference 20 were used for the calculation.

Table 2. NMR parameters calculated by PCM-n and PCM-m for Al at different T sites in MOR-4.7, MOR-5.6, and MOR-10

Parameter	Possible Al Site	MOR-4.7[a]		MOR-5.6[b]		MOR-10[b]	
		PCM-n[c]	PCM-m[d]	PCM-n[c]	PCM-m[d]	PCM-n[c]	PCM-m[d]
C_Q[e] (MHz)	T1	0.27	0.44	1.17	1.20	1.10	1.16
	T2	0.25	0.36	0.66	0.75	0.58	0.67
	T3	0.30	0.41	0.44	0.43	0.52	0.46
	T4	0.28	0.43	0.09	0.19	0.15	0.32
η[f]	T1	0.34	0.24	0.64	0.64	0.60	0.62
	T2	0.19	0.35	0.72	0.62	0.93	0.87
	T3	0.08	0.45	0.99	0.74	0.72	0.90
	T4	0.36	0.69	0.63	0.06	0.97	0.85
δ_{CG1}[g] (ppm)	T1	−31.2	−31.2	−31.7	−31.7	−31.6	−31.6
	T2	−29.1	−29.1	−30.5	−30.5	−30.5	−30.5
	T3	−30.2	−30.2	−30.0	−30.0	−29.9	−29.9
	T4	−30.6	−30.6	−30.2	−30.2	−30.4	−30.5
δ_{CG2}[h] (ppm)	T1	56.8	56.8	57.1	57.1	57.0	57.0
	T2	53.0	52.9	55.5	55.4	55.4	55.4
	T3	55.0	55.0	54.5	54.6	54.4	54.4
	T4	55.8	55.8	55.0	55.0	55.5	55.5

[a]The coordinates extracted from reference 19 were used for the calculation; [b]The coordinates extracted from reference 20 were used for the calculation; [c]The point charge of −1 for the nearest oxygen atoms was used to calculate the NMR parameter values by the PCM-n; [d]The point charge of −1 for oxygen the atoms in the first layer and the 3rd layer, and the point charge of +2 for silicon atoms in the second layer were used to calculate the NMR parameter values by the PCM-m; [e]Quadrupole coupling constant, [f]Asymmetry parameter for quadrupole interaction; [g]The shift of the center of gravity on the F1 axis; and [h]The shift of the center of gravity on the F2 axis.

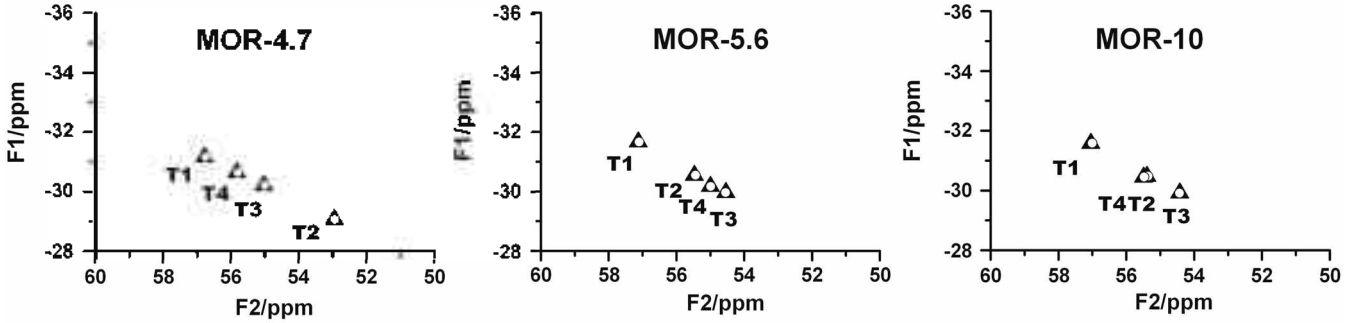

Figure 1. Comparison of peak positions for individual T sites in ^{27}Al MQMAS NMR spectra simulated by the PCM-n (▲) and the PCM-m (○) for MOR-4.7, MOR-5.6, and MOR-10: Point charge of -1 and 2 for O and Si, respectively, were used for the simulation.

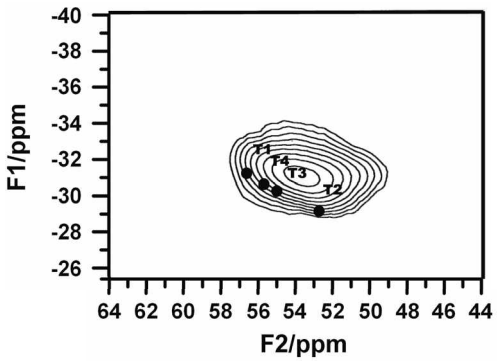

Figure 2. Experimental ^{27}Al MQMAS NMR spectrum of MOR-6.5(CBV10A) overlaid with the simulated peak positions obtained using the PCM-n method for MOR 4.7.

very little by C_Q.

The influence of the point charge variation at the oxygen and silicon sites on the ^{27}Al MQMAS NMR spectra simulated using the PCM-m method is shown in Figure 3, where the charge of oxygen was varied from −0.5 to −2 and that of silicon was varied from +0.5 to +4 in steps of 0.5. The data selected from the calculated parameters for MOR-5.6 which had the largest variation of the simulated spectra, are presented in Table 3 as representative data. In general, the peak positions move along the F2 axis over a wider range than along the F1 axis, which is to be expected since the effect of C_Q was scaled down by a factor of 10/31 along the F1 axis as expressed in the equation for δ_{CG1}. Another trend easily noticeable in Figure 3 is that the T1 peak positions changed more than the peak positions of the other T sites in the spectra. This indicates that the T1 sites are less spherical than the other T sites because the quadrupole parameters of the less spherical sites are more highly influenced by the charge variation. The spectra generated using the PCM-n method were also affected by the variation of the point

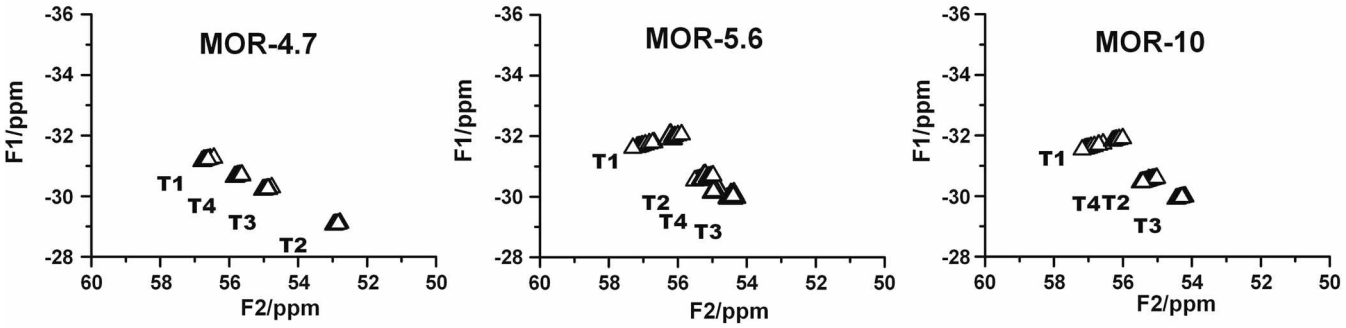

Figure 3. Influence of point charge on ^{27}Al MQMAS NMR spectra of MOR-4.7, MOR-5.6, and MOR-10 simulated by the PCM-m method. The point charges of O and Si were varied from −0.5 to −2 and 0.5 to 4, respectively, in steps of 0.5.

Table 3. Point charge influence on NMR parameters calculated by PCM-m for Al at different T sites in MOR-5.6

Parameter	Possible Al site	(−1)(X)(−1)[a]								(Y)(2)(Y)[b]			
		0.5	1	1.5	2	2.5	3	3.5	4	−0.5	−1	−1.5	−2
C_Q[c] (MHz)	T1	1.06	1.07	1.12	1.20	1.30	1.43	1.57	1.72	0.86	1.20	1.66	2.15
	T2	0.53	0.60	0.67	0.75	0.83	0.91	1.00	1.08	0.54	0.75	0.97	1.19
	T3	0.42	0.35	0.34	0.43	0.57	0.73	0.90	1.07	0.53	0.43	0.49	0.69
	T4	0.31	0.15	0.06	0.19	0.35	0.51	0.67	0.83	0.42	0.19	0.09	0.30
η[d]	T1	0.70	0.66	0.65	0.64	0.62	0.60	0.58	0.56	0.56	0.64	0.65	0.66
	T2	0.97	0.76	0.63	0.62	0.67	0.75	0.83	0.90	0.91	0.62	0.66	0.76
	T3	0.17	0.38	0.81	0.74	0.53	0.37	0.26	0.18	0.18	0.74	0.72	0.38
	T4	0.39	0.55	0.04	0.06	0.14	0.17	0.19	0.20	0.20	0.06	0.77	0.55
δ_{CG1}[e] (ppm)	T1	−31.6	−31.6	−31.7	−31.7	−31.7	−31.7	−31.8	−31.8	−31.6	−31.7	−31.8	−32.0
	T2	−30.5	−30.2	−30.5	−30.5	−30.6	−30.6	−30.6	−30.6	−30.5	−30.5	−30.6	−30.6
	T3	−30.0	−30.0	−30.0	−30.0	−30.0	−30.0	−30.0	−30.0	−30.0	−30.0	−30.0	−30.0
	T4	−30.2	−30.2	−30.2	−30.2	−30.2	−30.2	−30.2	−30.2	−30.2	−30.2	−30.2	−30.2
δ_{CG2}[f] (ppm)	T1	57.1	57.2	57.2	57.1	57.0	56.9	56.8	56.7	57.3.	57.1	56.7.	56.2
	T2	55.5	55.5	55.5	55.4	55.4	55.4	55.3	55.2	55.5	55.4	55.3	55.2
	T3	54.6	54.6	54.6	55.6	54.5	54.5	54.4	54.3	54.5	55.6	54.5	54.5
	T4	55.0	55.0	55.0	55.0	55.0	54.9	54.9	54.8	55.0	55.0	55.0	55.0

[a]The point charge for silicon site, X, was varied from 0.5 to 4 in steps of 0.5 while the point charge of oxygen site was fixed at −1; [b]The point charge for oxygen site, Y, was varied from −0.5 to −2 in steps of 0.5 while the point charge of silicon site was fixed at 2; [c]Quadrupole coupling constant; [d]Asymmetry parameter for quadrupole interaction; [e]The shift of the center of gravity on the F1 axis; and [f]The shift of the center of gravity on the F2 axis.

charges, in a similar manner to those generated using the PCM-m: the variation of the peak position was greater for the less spherical T sites.

To confirm the validity of the PCM-m method that we used, the results obtained from the HF calculation and the PCM-m method were compared. The chemical shifts calculated by the HF method were in the range of 89.2-90.2 ppm for T1, T2, and T4 sites and 95.4 ppm for the T3 sites. The charges calculated by the HF method were −1.4, +2.7, and −1.2 for the oxygen in the first layer, the silicon in the second layer, and the oxygen in the third layer, respectively. All of the chemical shifts determined by the HF method differed significantly from the observed values or the typical ones for the Al at the T sites in aluminum oxides. Thus, for δ_i, the values obtained from the average T-O-T angles, rather than the ones calculated by the HF method, were used to simulate the ^{27}Al MQMAS NMR spectra. In Table 4, the C_Q, η, δ_{CG1}, and δ_{CG2} values of MOR-4.7 obtained by the HF calculation and the PCM-m method, based on the same charge values obtained using the HF method, are compared side by side. In addition, the data from the PCM-m calculated with the charges of −1 for oxygen and +2 for silicon are shown. Even in the case where some of the C_Q and η values obtained by the HF and the PCM-m method were quite different, the δ_{CG1} and δ_{CG2} values calculated from the parameters were still similar. As a result, the simulated spectra were very similar in their patterns, as shown in Figure 4. This implies that the MQMAS NMR spectra are not sensitive to the quadrupole parameters, as long as the C_Q values are small. In our case, the C_Q values obtained using either the HF or the PCM were smaller than 1.5 MHz.

The calculation of quadrupole parameters by PCM methods has been mainly limited to well crystallized materials such as single crystals or crystalline thin layers, where an infinite array of atoms can be reasonably assumed for the calculation.[24] PCM methods have also been employed for the study of the chemicals wherein only the nearest neighbors

Table 4. Comparison of parameters for MOR-4.7 calculated by PCM-m and HF method

Parameters	Possible Al Site	PCM-m[a] (−1)(2)(−1)	PCM-m[b] (−1.4)(2.7)(−1.2)	HF[c] (−1.4)(2.7)(−1.2)
C_Q[d] (MHz)	T1	0.44	0.68	0.62
	T2	0.36	0.55	0.52
	T3	0.41	0.60	1.30
	T4	0.43	0.63	0.64
η[e]	T1	0.24	0.23	0.93
	T2	0.35	0.35	0.58
	T3	0.45	0.62	0.81
	T4	0.69	0.83	0.37
δ_{F1}[f] (ppm)	T1	−31.2	−31.2	−31.2
	T2	−29.1	−29.1	−29.1
	T3	−30.2	−30.2	−30.4
	T4	−30.6	−30.7	−30.7
δ_{F2}[g] (ppm)	T1	56.8	56.7	56.7
	T2	52.9	52.9	52.8
	T3	55.0	55.0	54.5
	T4	55.8	55.7	55.7

[a]The point charges of 2 and −1 for silicon and oxygen sites, respectively, and the coordinates extracted from reference 19 were used to calculate the parameters by the PCM-m method; [b]The point charges of −1.4, 2.7, and −1.2, for the nearest 4 oxygen atoms, 4 silicon atoms connected to the 4 oxygen atoms, and 12 additional oxygen atoms bonded to the silicon atoms, respectively, and the coordinates extracted from reference 19 were used to calculate the parameters by the PCM-m method; [c]From the HF method, the charges, −1.4, 2.7, and −1.2, were estimated for the nearest 4 oxygen atoms, 4 silicon atoms connected to the 4 oxygen atoms, and 12 additional oxygen atoms bonded to the silicon atoms, respectively; [d]Quadrupole coupling constant; [e]Asymmetry parameter for quadrupole interaction; [f]The shift of the center of gravity on the F1 axis; and [g]The shift of the center of gravity on the F2 axis.

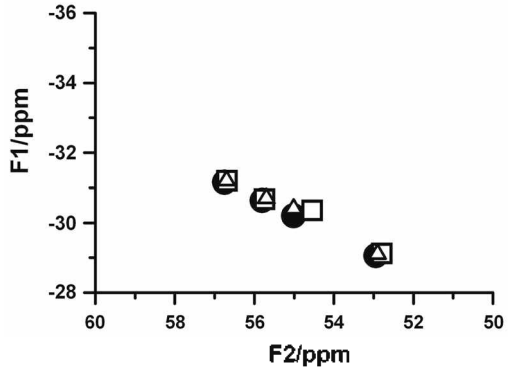

Figure 4. Comparison of peak positions for each T site in ^{27}Al MQMAS NMR spectra of MOR-4.7 obtained by the PCM-m and the HF. The coordinates from reference 19 were used for the peak position calculation. Peak positions estimated by the PCM-m method with the point charges of 2 and −1 for silicon and oxygen, respectively, are denoted by ●. The peak positions estimated by the PCM-m method with the point charge of −1.4, 2.7, and −1.2, for the nearest 4 oxygen atoms, 4 silicon atoms connected to the 4 oxygen atoms, and 12 additional oxygen atoms bonded to the silicon atoms, respectively, are denoted by △. The peak positions estimated by the HF method are marked with □. From the HF method, the charge, −1.4, 2.7, and −1.2, were estimated for the nearest 4 oxygen atoms, 4 silicon atoms connected to the 4 oxygen atoms, and 12 additional oxygen atoms bonded to the silicon atoms, respectively.

are structurally well defined.[25] Porous materials can be crystalline but, due to the many pores within them, they have many dangling bonds which are not far away from the atomic sites being considered. Therefore, if the PCM-n were good enough to predict the ^{27}Al MQMAS NMR spectra, it would be useful, especially for porous materials. At the same time, it can be rationalized that acquiring ^{27}Al MAS spectra at higher magnetic fields rather than carrying out MQMAS NMR experiments would provide a simpler way of resolving peaks corresponding to the different Al sites with small C_Q values, unless the chemical shift distribution for each Al site is wide enough to nullify the higher spectral resolution expected at the higher magnetic fields.

The local structures of the specific T sites were observed to change when the Si/Al ratio of MOR varied, but no systematic correlation between the Si/Al ratio and the local structures of the T sites was detected.[19,20,26-31] This suggests that the local structures of MOR are not only sensitive to the Si/Al ratio, but also equally or more so to other factors such as defect sites and non-frame cations.

Conclusions

The PCM calculation is simple and convenient to use and does not require sophisticated and expensive computer programs along with specialists to run them. Nevertheless, in this study, the PCM calculation generated peak positions in the ^{27}Al MQMAS NMR spectra of MOR reasonably, as compared with the HF method. In addition, the spectra generated by the PCM-n and the PCM-m did not differ from each other. This suggests that the PCM-n, in which only the nearest neighbor atoms are taken into account in the calculation, is good enough to simulate the ^{27}Al MQMAS NMR spectra of MOR. However, it should be pointed out that this might apply only for the Al sites with small quadrupole coupling constants. Thus, the PCM-n method is expected to be useful for the preliminary simulation of the ^{27}Al MQMAS spectra of porous materials which have large unit cells and high volume densities of pores but relatively small C_Q values for the Al sites. The tolerance of the PCM-n against the size of C_Q will be reported in the near future.

Acknowledgements. This work was supported by the Korea Research Council of Fundamental Science and Technology through grants, B2631B, B2731B, PG2313 and C22025, at the KBSI. We wish to thank Professor Woo Taik Lim at the Andong University for helping us to learn how to use the Ortep program, which was used to extract the coordinates of the neighboring atoms in the initial stage of the simulation.

References

1. Burbidge, B. W.; Keen, I. M.; Eyles, M. K. In *Advances in Chemistry Series, Molecular Sieve Zeolites, Physical and Catalytic Properties of Zeolite Modernite*; Flanigen, E. M., Sand, L. B., Eds.; American Chemical Society: Washington, 1971; Vol 101-102, p 400.

2. Engelhardt, G.; Michel, D. *High Resolution Solid State NMR of Silicates and Zeoltes*; John Wiley & Sons: New York, 1987.
3. Klinowski, J. *Chem. Rev.* **1991**, *91*, 1459.
4. Fyfe, C. A.; Feng, Y.; Grondey, H.; Kokotailo, G. T.; Gies, H. *Chem. Rev.* **1991**, *91*, 1525.
5. Barras, J.; Klinowski, J. *J. Chem. Soc. Faraday Trans.* **1994**, *90*, 3719.
6. Fernandez, C.; Amoureux, J. P. *Chem. Phys. Lett.* **1995**, *242*, 449.
7. Baltisberger, J. H.; Xu, Z.; Stebbins, J. F.; Wang, S. H.; Pines, A. *J. Am. Chem. Soc.* **1996**, *118*, 7209.
8. Ashbrook, S. E.; McManus, J.; MacKenzie, K. J. D.; Wimperis, S. *J. Phys. Chem. B* **2000**, *104*, 6408.
9. Chen, T. H.; Wouter, B. H.; Grobet, P. J. *Eur. J. Inorg. Chem.* **2000**, 281.
10. Chen, J.; Chen, T.; Guan, N.; Wang, J. *Catal. Today* **2004**, *93-95*, 627.
11. Han, O. H.; Kim, C. S.; Hong, S. B. *Angew. Chem. Int. Ed.* **2002**, *41*, 469.
12. Frydman, L.; Harwood, J. S. *J. Am. Chem. Soc.* **1995**, *117*, 5367.
13. Medek, A.; Harwood, J. S.; Frydman, L. *J. Am. Chem. Soc.* **1995**, *117*, 12779.
14. Mains, G. J.; Nantsis, E. A.; Carper, W. R. *J. Phys. Chem. A* **2001**, *105*, 4371.
15. Gauss, J.; Schneider, U.; Ahlrichs, R.; Dohmeier, C.; Schnöckel, H. *J. Am. Chem. Soc.* **1993**, *115*, 2402.
16. Koller, H.; Meijer, E. L.; van Santen, R. A. *Solid State NMR* **1997**, *9*, 165.
17. Chem, L.; Zhan, M.; Yue, Y.; Ye, C.; Deng, F. *Micropor. Mesopor. Mater.* **2004**, *76*, 151.
18. Valiyev, K. A.; Zripov, M. M. *Zh. Strukt. Khim.* **1966**, *7*, 494.
19. Schlenker, J. L.; Pluth, J. J.; Smith, J. V. *Mat. Res. Bull.* **1979**, *14*, 849.
20. Martucci, A.; Gruciani, G.; Alberti, A.; Ritter, C.; Ciambelli, P.; Rapacciuolo, M. *Micropor. Mesopor. Mater.* **2000**, *35-36*, 405.
21. Lippmaa, E.; Samoson, A.; Mägi, M. *J. Am. Chem. Soc.* **1986**, *108*, 1730.
22. Frisch, M. J. *et al. Gaussian 98*, Rev. A.7; Gaussian Inc.: Pittsburgh, PA, 1998.
23. Man, P. P. *Phys. Rev. B* **1998**, *58*, 2764.
24. Park, I. W.; Choi, H.; Kim, H. J.; Shin, H. W.; Park, S. S.; Choh, S. H. *Phys. Rev. B* **2002**, *65*, 195210.
25. Han, O. H.; Oldfield, E. *Inorg. Chem.* **1990**, *29*, 3667.
26. Mortier, W. J.; Pluth, J. J.; Smith, J. V. *Mat. Res. Bull.* **1975**, *10*, 1037.
27. Schelenker, J. L.; Pluth, J. J.; Smith, J. V. *Mat. Res. Bull.* **1978**, *13*, 77.
28. Schelenker, J. L.; Pluth, J. J.; Smith, J. V. *Mat. Res. Bull.* **1978**, *13*, 169.
29. Schelenker, J. L.; Pluth, J. J.; Smith, J. V. *Mat. Res. Bull.* **1978**, *13*, 901.
30. Schelenker, J. L.; Pluth, J. J.; Smith, J. V. *Mat. Res. Bull.* **1979**, *14*, 751.
31. Ito, M.; Saito, Y. *Bull. Chem. Soc. Jpn.* **1985**, *58*, 3035.